ELSEVIER

Thermochimica Acta 322 (1998) 137–151

thermochimica acta

# Thermogravimetric study of the dehydration process of α-cyclodextrin: comparison between conventional and high-resolution TGA

V. Berbenni*, A. Marini, G. Bruni

*C.S.G.I. Dipartimento di Chimica Fisica dell'Università di Pavia, Viale Taramelli, 16-27100 Pavia, Italy*

Received 22 May 1998; received in revised form 2 July 1998; accepted 6 July 1998

**Abstract**

The aim of resolving the several steps of α-cyclodextrin (αCD) dehydration has been pursued, both by conventional (constant heating rate) and high-resolution TGA. It is shown that a careful selection of the experimental parameters (heating rate and resolution parameters) in both TGA modes leads to very similar results. In particular, it has been demonstrated that four steps can be resolved in the TGA curves. Stage 1 is due to surfacial water release. Stages 2 and 3 correspond to the water present in the interstices. Stage 4 individuates the water inside the αCD cavity. © 1998 Elsevier Science B.V.

*Keywords:* Dehydration; High-resolution TGA; TGA; α-Cyclodextrin

## 1. Introduction

Cyclodextrins are cyclic oligosaccharides which form complexes with water and many organic molecules [1]. In the previous works published by our group on cyclodextrins, attention was mainly focused on the hydration/dehydration thermodynamics of the β form. In particular, we showed that a structural transformation takes place during dehydration [2]. Then, we discussed in detail the role of such a transformation and brought into evidence that it is strictly linked to dehydration [3]. Finally, a detailed discussion was presented on thermal measurements (DSC) whereby it was deduced that the enthalpy associated with the structural transformation contributes substantially to the DSC peak usually assigned to the β-cyclodextrin dehydration [4]. Recently, we have initiated an analysis of the thermodynamics of hydration/dehydration of the other two natural forms of cyclodextrin, namely α-cyclodextrin and γ-cyclodextrin. Here, the first results of such a study are reported, concerned with the dehydration process of α-cyclodextrin (αCD in the following). As the process is constituted by several consecutive steps, we will try and separate the different dehydration stages, both by conventional thermogravimetric analysis and high-resolution thermogravimetry. Therefore, the results, besides their scientific interest in the field of cyclodextrins, will constitute, in our opinion, a significant test of the reliability of high resolution TGA (Hi-Res™, patent pending) in the separation of closely occurring thermal events.

*Corresponding author.


PII: S0040-6031(98)00484-5

## 2. Experimental

### 2.1. Products

αCD was kindly provided by Wacker Chemie Italy. Its nominal composition was $\alpha CD \cdot 6H_2O$. The sample has been examined as received.

### 2.2. Apparatus and procedures

TGA measurements have been performed by a TGA 2950 thermogravimetric analyzer (TA Instruments, USA) connected with a TA3100 Computer (also by TA Instruments) to store and analyze the data (Thermal Solutions™ software). All the measurements have been performed under a flow of nitrogen (100 ml/min) bubbled through water at room temperature (rt in the following). The samples (ca. 15 mg) were scanned between rt and 160°C.

Three different types of experimental approach have been utilized:

*Constant heating rate TGA*: this is the conventional TGA approach and the measurements have been performed at heating rates ($\beta$) of 0.2, 0.5, 1, 2, 5 and 10°C/min;

*Dynamic rate high-resolution TGA*: this is the first choice Hi-Res TGA mode. The heating rate of the sample is dynamically and continuously varied in response to changes in the sample's rate of mass change so as to maximize mass resolution. The allowed values of resolution parameter ($R$) vary between 2 (loose control) and 8 (strict control). We have used $R$ values ranging between 2 and 6 (in steps of 1) with nominal heating rates of 5 and 10°C/min. This mode usually provides good results with temperature-separable transformations;

*Constant reaction rate high-resolution TGA*: in the constant reaction rate approach the heater control system varies the temperature of the furnace as required to maintain a constant preselected rate of mass change (%/min) . Whenever the rate of weight change exceeds the threshold value, the heating rate is reduced, even to the point of cooling. When %/min falls below the threshold, the heating rate is increased up to the maximum value specified for the ramp segment. In this approach, moderate heating rates work best, as this can avoid excessive reaction rates and temperature overshoots. Resolution parameter values are negative, and in the present study they have been set as indicated in the table reported below.

| $R$ | Threshold/(%/min) | $\beta$/(°C/min) |
|---|---|---|
| −4.4 | 0.20 | 1 – 2 |
| −4.0 | 0.32 | 1 – 2 – 5 |
| −3.6 | 0.50 | 1 – 2 – 5 |
| −3.3 | 0.71 | 1 – 2 – 5 |
| −3.0 | 1.00 | 1 – 2 – 5 |
| −2.7 | 1.40 | 1 – 2 – 5 |

## 3. Results and discussion

### 3.1. Constant heating-rate thermogravimetry

Table 1 reports the results obtained with the conventional TGA technique at different heating rates. The data represent the mean values of three independent runs performed at each heating rate. Four different dehydration stages can be individuated on the basis

Table 1
Conventional TGA results. $\beta$ is the heating rate (°C/min); $m_0$ the initial mass gain (%); $\Delta m_n$ ($n$=1 to 4) represent the relative mass losses of the different dehydration stages and have to be intended as negative values expressed in %; $T_n$ ($n$=1 to 4) represent the final temperatures of the dehydration stages expressed in °C; $\Delta m_t$ the total mass loss (negative value in %) recorded in the run; $\Delta m_{2+3}$ the relative mass loss of stages 2+3; $\Delta m_{4\rightarrow}$ the relative mass loss from the beginning of stage 4 up to the end of the measurement ($T$=160°C)

| $\beta$ | $m_0$ | $\Delta m_1$ | $T_1$ | $\Delta m_2$ | $T_2$ | $\Delta m_3$ | $T_3$ | $\Delta m_{2+3}$ | $\Delta m_4$ | $T_4$ | $\Delta m_{4\rightarrow}$ | $\Delta m_t$ |
|---|---|---|---|---|---|---|---|---|---|---|---|---|
| 0.2 | +0.5 | 1.22 | 46.0 | 2.45 | 57.6 | 4.00 | 83.3 | 6.45 | 1.63 | 94.9 | 2.92 | 10.59 |
| 0.5 | +0.6 | 1.14 | 45.7 | 2.51 | 58.5 | 3.97 | 83.0 | 6.48 | 1.49 | 92.7 | 2.82 | 10.44 |
| 1.0 | +0.4 | 1.13 | 47.6 | 2.65 | 63.2 | 3.84 | 85.5 | 6.49 | 1.59 | 98.0 | 2.78 | 10.40 |
| 2.0 | +0.3 | 1.11 | 49.8 | 2.83 | 68.6 | 3.67 | 90.2 | 6.50 | 1.74 | 104.9 | 2.81 | 10.42 |
| 5.0 | +0.2 | 0.83 | 48.8 | 3.12 | 73.3 | 3.40 | 93.3 | 6.52 | 1.99 | 110.8 | 2.85 | 10.20 |
| 10.0 | +0.1 | 0.89 | 51.3 | 3.25 | 78.3 | 3.29 | 97.4 | 6.54 | 2.07 | 115.2 | 2.84 | 10.27 |

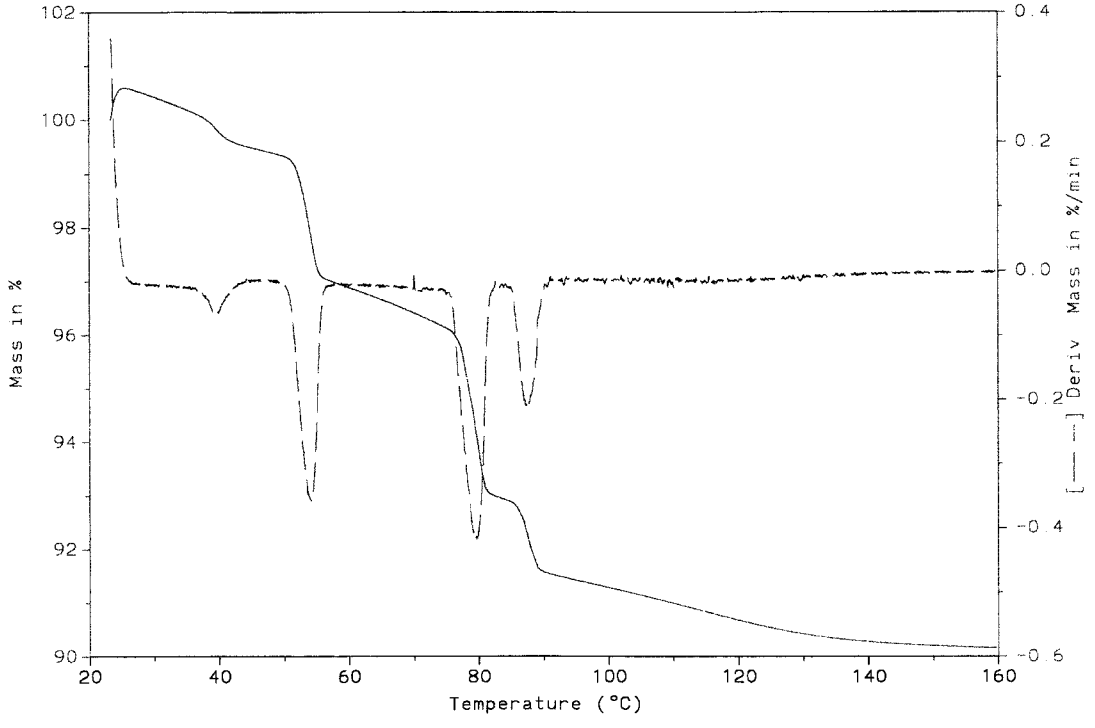


Fig. 1. TGA scan of αCD (conventional mode). % Mass and derivative mass (%/min) vs. temperature (°C). Heating rate, 0.5°C/min.

of the DTG peaks as represented in Fig. 1 that reports, as an example, a TGA run performed at 0.5°C/min. After the fourth stage is completed, a continuous mass loss occurs which ends near the maximum run temperature (ca. 160°C).

The second column of Table 1 reports the initial mass gain, whose presence indicates that the $\alpha CD{\cdot}6H_2O$ formula does not represent the saturated composition under the adopted experimental conditions of relative humidity. The initial water intake decreases on increasing the heating rate, as the equilibration process is not an instantaneous one. The first dehydration stage ($\Delta m_1$) includes this initial water intake and does not show a pronounced dependence on heating rate as long as the initial intake does not. By noting that the final temperature of the stage is only slightly scattered around a rather low mean value ($T_1$=48.2±2.2°C), it is reasonable to conclude that the first stage involves 'surface' water, part of which is absorbed in the early stage of the run. In our experimental conditions, surface water can reach an amount of 1.22% by mass. The mass loss relevant to the second stage ($\Delta m_2$) and its final temperature ($T_2$) show a definite tendency to increase on increasing the heating rate. However, $\Delta m_3$ (third stage) shows the opposite trend. The result is that $\Delta m_{2+3}$ is independent of the heating rate ($\Delta m_{2+3}$=6.50±0.03%), despite the fact that the final temperature of stage 3 ($T_3$) increases with heating rate. It seems that stages 2 and 3 can be reliably resolved by conventional TGA only for $\beta \leq 0.5$°C/min ($\Delta m_2$=2.48±0.04% , $\Delta m_3$= 3.99±0.02%). The same is true for stage 4 and for the following continuous mass loss: they show the same heating rate dependence discussed for stages 2 and 3, respectively. In this instance, the overall mass change is $\Delta m_{4\rightarrow}$=2.84±0.05%. Stage 4 is well resolved by conventional TGA only at low heating rates, where the relative mass loss is $\Delta m_{4\rightarrow}$=1.57± 0.07%. Thus, depending on the heating rate utilized, three (1, 2+3, 4→ at $\beta \geq 1$°C/min) or four (1 through 4 at $\beta \leq 0.5$°C/min) stages can be reliably separated in the dehydration process. It seems this is a promising case study, where the real effectiveness of high-resolution thermogravimetry can be verified. It has to be

Table 2
Dynamic rate Hi–Res™ TGA results. The symbols stand for the same quantities as in Table 1. *R* represents the resolution parameter (see text)

| R | $\beta$ | $m_0$ | $\Delta m_1$ | $T_1$ | $\Delta m_2$ | $T_2$ | $\Delta m_3$ | $T_3$ | $\Delta m_{2+3}$ | $\Delta m_4$ | $T_4$ | $\Delta m_{4\rightarrow}$ | $\Delta m_t$ |
|---|---|---|---|---|---|---|---|---|---|---|---|---|---|
| 2 | 5 | +0.2 | 0.88 | 49.6 | 3.01 | 74.1 | 3.56 | 92.7 | 6.57 | 1.84 | 107.1 | 2.81 | 10.26 |
| 2 | 10 | +0.2 | 0.86 | 51.5 | 3.25 | 79.1 | 3.13 | 98.6 | 6.38 | 2.26 | 116.2 | 2.96 | 10.20 |
| 3 | 5 | +0.1 | 0.77 | 48.5 | 2.93 | 68.1 | 3.73 | 90.1 | 6.66 | 1.64 | 103.0 | 2.72 | 10.15 |
| 3 | 10 | +0.1 | 0.71 | 51.4 | 3.22 | 78.4 | 3.05 | 97.1 | 6.27 | 2.33 | 114.5 | 3.05 | 10.03 |
| 4 | 5 | +0.1 | 0.76 | 47.2 | 2.70 | 62.1 | 4.02 | 87.1 | 6.72 | 1.44 | 97.4 | 2.68 | 10.16 |
| 4 | 10 | +0.1 | 0.58 | 48.2 | 2.84 | 68.7 | 3.59 | 91.8 | 6.43 | 1.93 | 106.4 | 2.89 | 9.90 |
| 5 | 5 | +0.3 | 0.88 | 47.2 | 2.59 | 59.0 | 4.08 | 86.2 | 6.67 | 1.47 | 95.1 | 2.75 | 10.30 |
| 5 | 10 | +0.1 | 0.56 | 45.8 | 2.54 | 59.5 | 3.93 | 85.9 | 6.47 | 1.67 | 97.2 | 2.75 | 9.78 |
| 6 | 5 | +0.3 | 0.96 | 46.6 | 2.48 | 56.4 | 4.00 | 82.4 | 6.48 | 1.61 | 93.5 | 2.92 | 10.36 |
| 6 | 10 | +0.6 | 1.17 | 46.8 | 2.42 | 56.6 | 4.12 | 82.3 | 6.54 | 1.49 | 91.2 | 2.79 | 10.50 |

noted, for the sake of completeness, that a further mass loss process is set up in αCD at ca. 270°C, i.e. very close to the decomposition temperature [5]. Indeed, we continued the heating in some cases up to high temperature and confirmed, by FT-IR analysis of the evolved gas, that around 270°C, αCD undergoes a mass loss step ($\Delta m$=1.20±0.20%) where water is released [6]. As a matter of fact, we did not perform high-resolution TGA measurements up to such high temperatures, since no resolution problem concerning this dehydration stage is present.

### 3.2. Dynamic rate high resolution thermogravimetry

Table 2 reports the results obtained in the case of dynamic-rate approach (resolution parameter value $R$=2 to 6, $\beta$=5 and 10°C/min). Fig. 2(a) and (b) report the mass signal, its derivative with respect to time and the sample actual heating rate vs. temperature in two limiting cases (Fig. 2(a): $R$, 3; $\beta$, 10°C/min. Fig. 2(b): $R$, 5; $\beta$, 10°C/min). As it can be seen, the dynamic heating rate depends strongly on $R$ value: the minimum heating rate over stages 2, 3 and 4 is ca. 7°C/min for $R$=3 (Fig. 2(a)) while it is around 1°C/min for $R$=5 (Fig. 2(b)).

On examining the data of Table 2, the following considerations apply:

(a) only in a single case ($R$=6, $\beta$=10°C/min), a $\Delta m_1$ value is obtained (1.17%) which is nearly the same as the values found in conventional measurements performed at low heating rates. This is why, only in the case where the maximum resolution parameter is applied ($R$=6), the dynamic heating rate over stage 1 falls at a sufficiently low value (Fig. 3);
(b) so far as stages 2, 3 and 4 are concerned, it can be seen that their separation depends on $R$ (and, hence, on the related dynamic heating rate). For high $R$ values ($R$=5, 6), the relative mass losses of these stages are nearly the same as those obtained in the conventional runs carried out at $\beta \leq 0.5$°C/min. On the contrary, for low $R$ values ($R \leq 4$), they are quite different and only the overall mass losses $\Delta m_{2+3}$ and $\Delta m_{4\rightarrow}$ appear to be fairly reproducible.

It can be concluded that all the dehydration stages can be separated by dynamic rate measurements with $R \geq 5$. At the end of this section, a table will be reported reviewing, for the sake of clarity, the situation in regard to the results obtained by the different experimental approaches. Such a table will show that a clear advantage of the dynamic approach over the conventional one is that separation can be accomplished in a much shorter time.

### 3.3. Constant reaction rate high-resolution thermogravimetry

Fig. 4(a–f) report the mass signal, its derivative with respect to time and the actual heating rate vs. temperature for measurements performed under different values of the resolution parameter, but at the same heating rate (1°C/min). Fig. 4(g) reports, for the sake of comparison, the same signals as obtained in a conventional run performed at the same heating rate. On each figure, the maximum rates of mass loss of stages 1 through 4 are also reported.

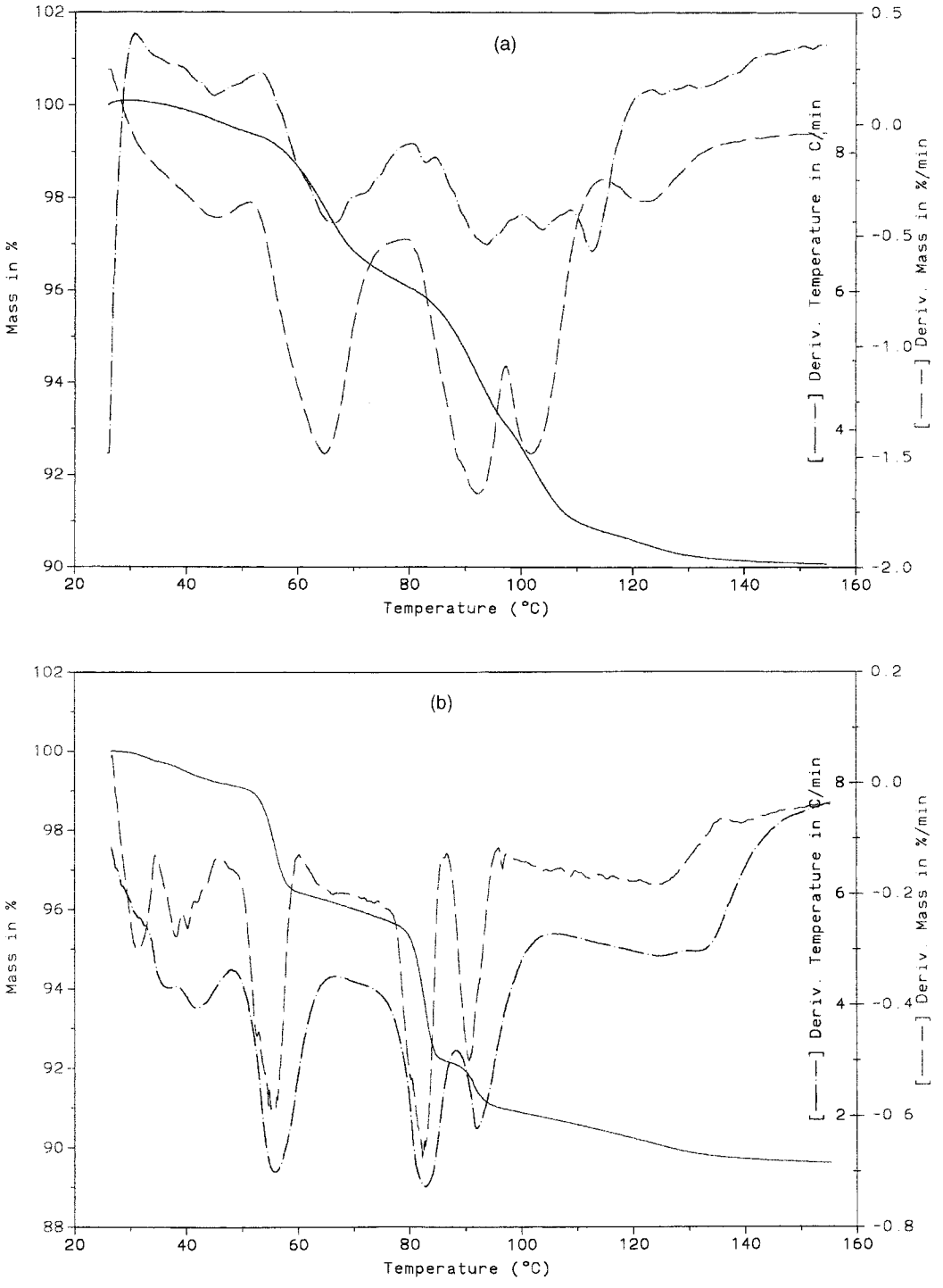


Fig. 2. (a) TGA scan of $\alpha$CD (high-resolution dynamic rate mode). % Mass, derivative mass (%/min) and dynamic heating rate (°C/min).Resolution parameter, $R$=3.0. Nominal heating rate, 10°C/min. (b) TGA scan of $\alpha$CD (high-resolution dynamic rate mode). % Mass, derivative mass (%/min) and dynamic heating rate (°C/min). Resolution parameter, $R$=5.0. Nominal heating rate, 10°C/min.

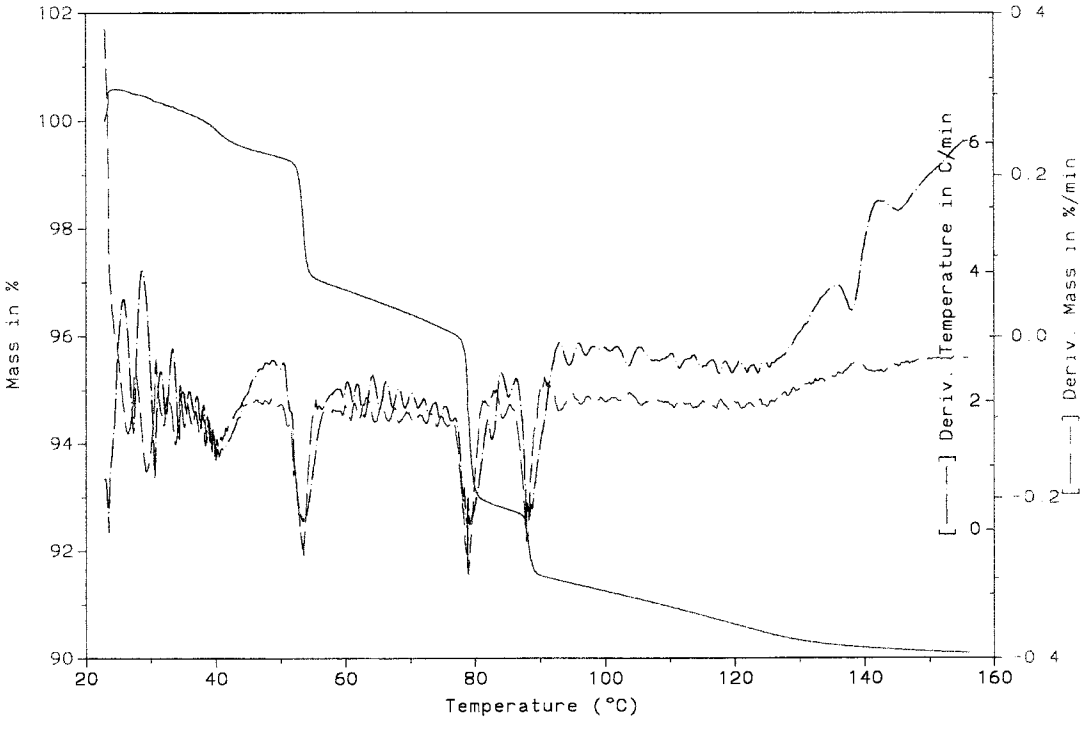


Fig. 3. TGA scan of αCD (high-resolution dynamic rate mode). % Mass, derivative mass (%/min) and dynamic heating rate (°C/min). Resolution parameter, $R$=6.0; and nominal heating rate, 10°C/min.

It can be seen that the maximum rates of stages 2, 3 and 4 decrease on decreasing $R$. This is due to the decrease of the actual heating rate operated by the high-resolution algorithm (see the temperature derivative curves of Fig. 4(a–f).

On the contrary, the maximum rate of stage 1 remains unaffected with respect to what happens in the conventional run until an $R$ value of −4.4 is applied.

The behaviour described so far is quite unexpected if we recall what has been said in Section 2 on the constant reaction rate mode. Here, we see that the high resolution becomes operative also when the threshold imposed (by the $R$ parameter) to the mass loss rate is sensibly above the maximum values reached over the different dehydration stages (see, in particular, Fig. 4(a–c).

Fig. 5(a–e) report the same signals of Fig. 4 for measurements performed with a nominal heating rate of 5°C/min. The curves corresponding to the conventional run are reported in Fig. 5(f). Again, on each figure, the maximum rates of weight loss for stages 1 to 4 are reported.

In this case too the maximum rates of stages 2, 3 and 4 decrease on decreasing $R$ as a result of the high-resolution intervention (see the derivative temperature curves). Concerning stage 1, a decrease of the actual heating rate and, hence, of the maximum rate of mass loss is operative, starting from $R$=−3.0 downwards. Fig. 5(e) shows the instrumental response in the case where an exceedingly strict control has been imposed on the heating rate.

The general indication is that, under the constant reaction-rate mode, the high-resolution control is even more strict than it was anticipated in the experimental section (and stated by the Manufacturer). This question deserves to be further analyzed. However we will no longer dwell on it in this paper.

Let us now examine, in more detail, the results obtained by this mode (see Table 3). The following considerations can be made:

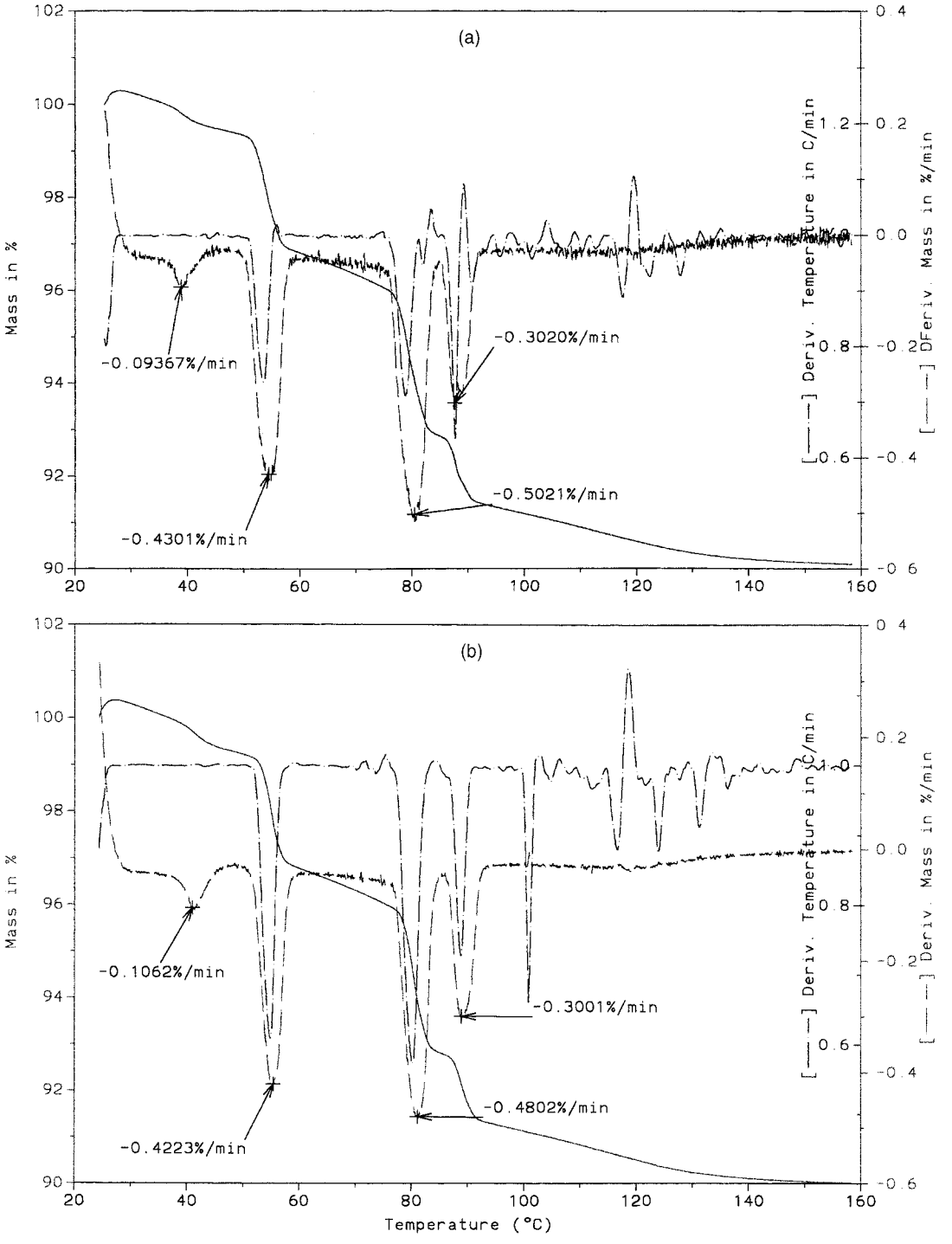


Fig. 4. TGA scans of αCD (high-resolution constant reaction-rate mode). % Mass, derivative mass (%/min) and dynamic heating rate (°C/min). Resolution parameter: $R$=−2.7(a); −3.0(b); −3.3(c); −3.6(d); −4.0(e); −4.4(f). Nominal heating rate: 1°C/min. (g) A conventional TGA scan at 1°C/min.

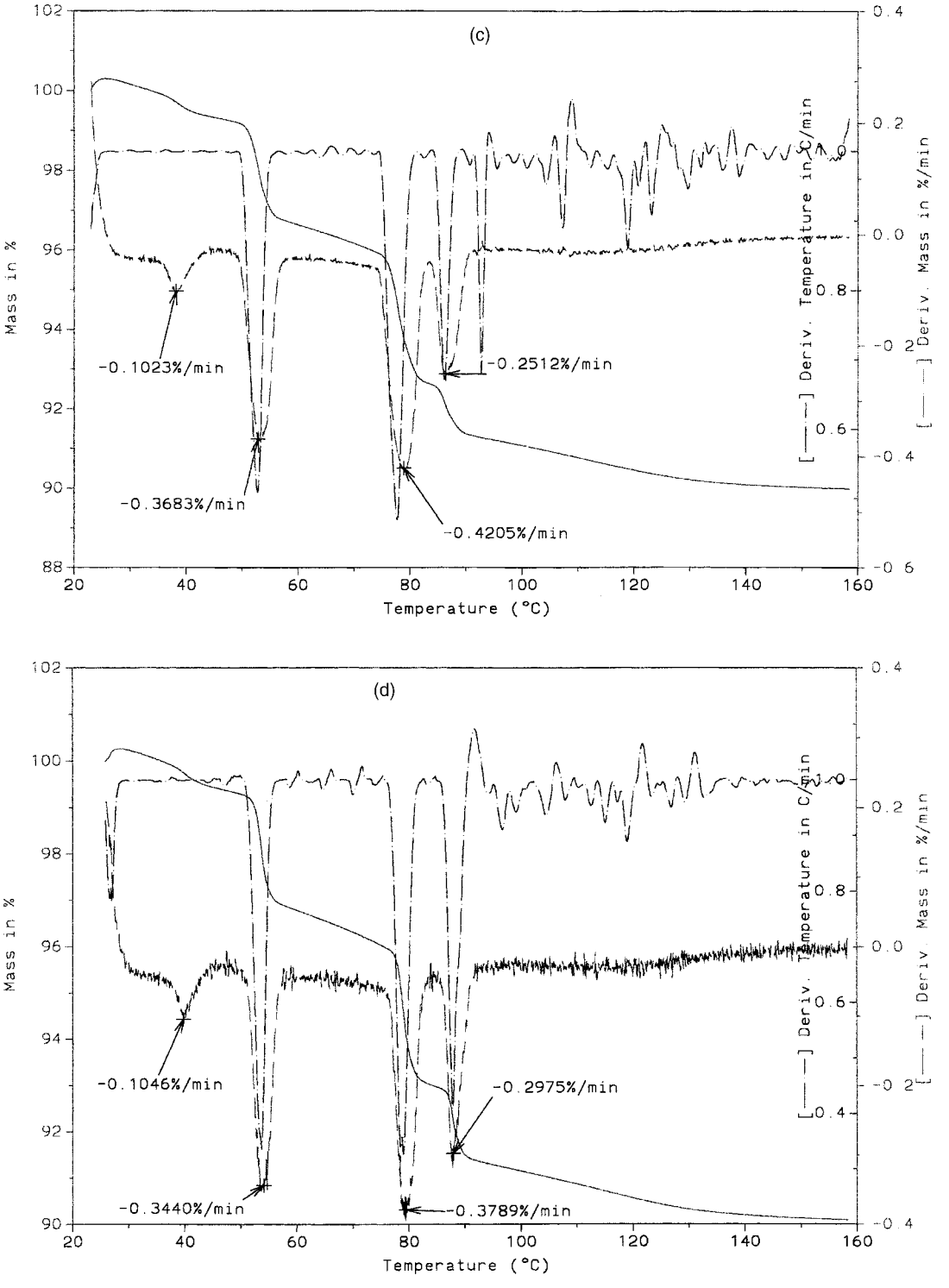


Fig. 4. *(Continued)*

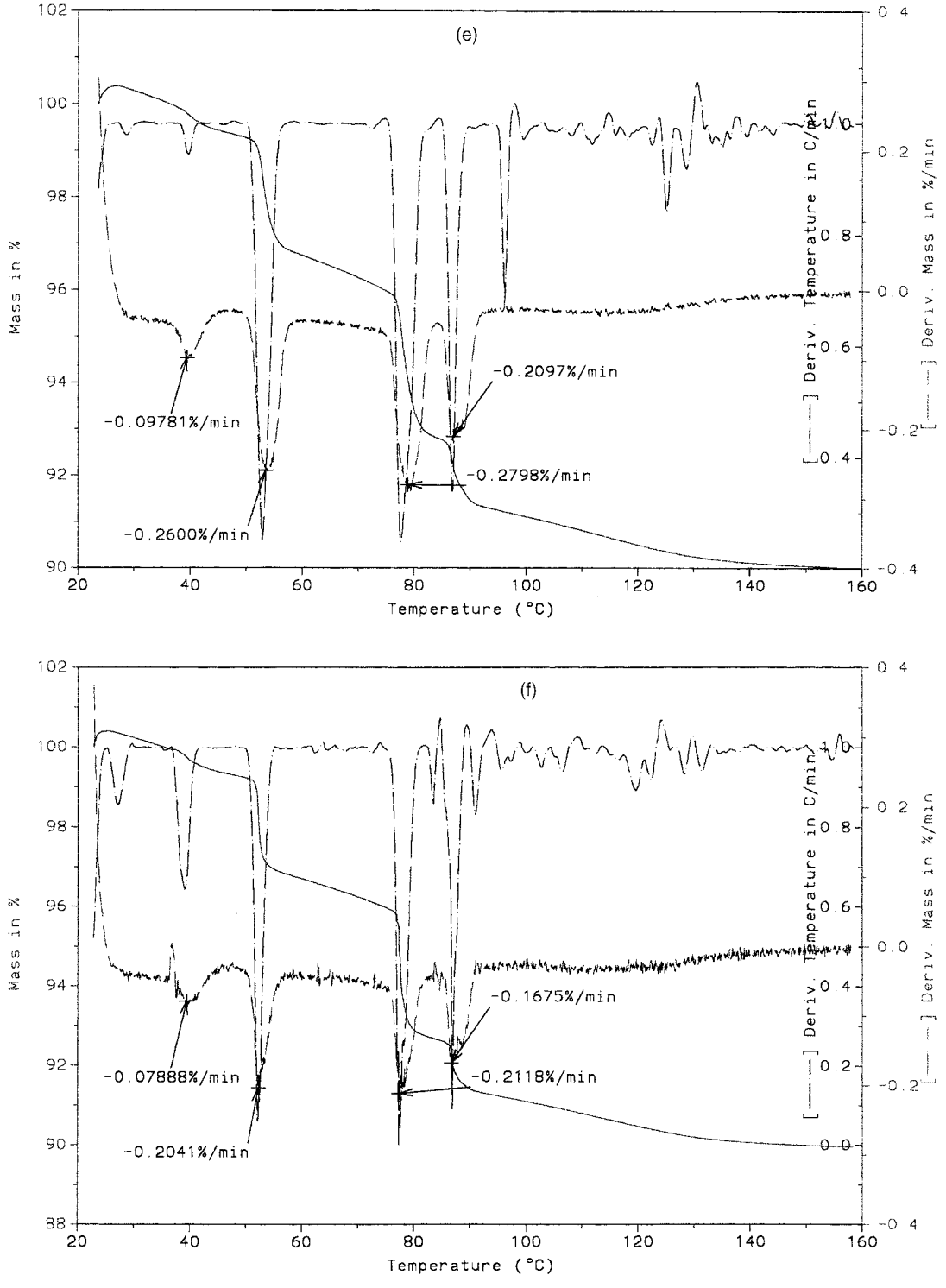


Fig. 4. *(Continued)*

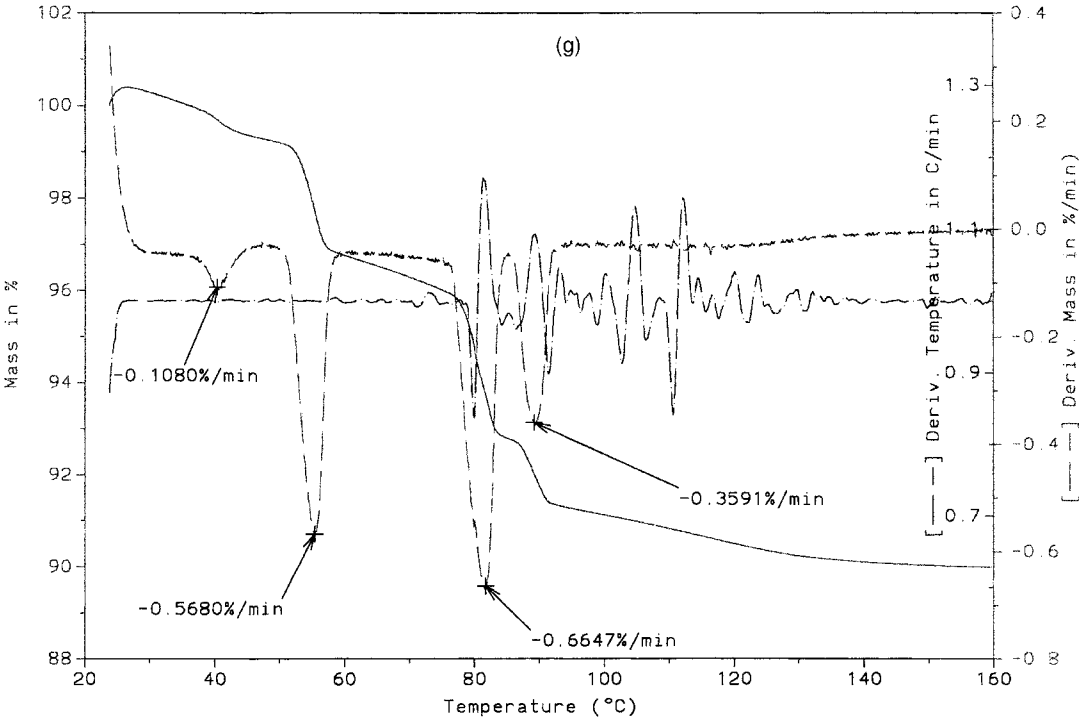


Fig. 4. (*Continued*)

Table 3
Constant reaction-rate Hi-Res™ TGA results. The symbols stand for the same quantities as in Table 1. *R* is the resolution parameter (see text)

| *R* | $\beta$ | $m_0$ | $\Delta m_1$ | $T_1$ | $\Delta m_2$ | $T_2$ | $\Delta m_3$ | $T_3$ | $\Delta m_{2+3}$ | $\Delta m_4$ | $T_4$ | $\Delta m_{4\rightarrow}$ | $\Delta m_t$ |
|---|---|---|---|---|---|---|---|---|---|---|---|---|---|
| −2.7 | 1 | 0.3 | 1.09 | 47.3 | 2.66 | 61.0 | 3.90 | 84.8 | 6.56 | 1.51 | 93.9 | 2.61 | 10.26 |
| −2.7 | 2 | 0.3 | 1.01 | 48.4 | 2.64 | 62.6 | 3.92 | 86.3 | 6.56 | 1.57 | 98.9 | 2.75 | 10.32 |
| −2.7 | 5 | 0.2 | 0.87 | 50.7 | 2.86 | 69.1 | 3.62 | 92.4 | 6.48 | 1.99 | 109.7 | 2.88 | 10.23 |
| −3.0 | 1 | 0.4 | 1.12 | 48.0 | 2.58 | 61.6 | 3.92 | 85.8 | 6.50 | 1.51 | 95.1 | 2.77 | 10.39 |
| −3.0 | 2 | 0.3 | 1.08 | 49.0 | 2.60 | 62.6 | 3.96 | 87.5 | 6.56 | 1.56 | 98.5 | 2.77 | 10.41 |
| −3.0 | 5 | 0.1 | 0.67 | 47.2 | 2.89 | 67.5 | 3.70 | 91.3 | 6.59 | 1.92 | 108.2 | 2.84 | 10.10 |
| −3.3 | 1 | 0.3 | 1.00 | 45.8 | 2.67 | 60.1 | 4.00 | 83.6 | 6.67 | 1.40 | 94.9 | 2.64 | 10.31 |
| −3.3 | 2 | 0.3 | 0.80 | 47.1 | 2.73 | 62.0 | 3.88 | 85.7 | 6.61 | 1.61 | 96.9 | 2.82 | 10.23 |
| −3.3 | 5 | 0.1 | 0.64 | 46.3 | 2.60 | 61.5 | 3.90 | 85.5 | 6.50 | 1.92 | 106.4 | 2.87 | 10.01 |
| −3.6 | 1 | 0.3 | 1.07 | 45.4 | 2.59 | 58.9 | 3.84 | 84.7 | 6.43 | 1.61 | 96.8 | 2.76 | 10.26 |
| −3.6 | 2 | 0.2 | 0.70 | 47.6 | 2.69 | 61.7 | 3.81 | 85.7 | 6.50 | 1.76 | 99.1 | 2.84 | 10.04 |
| −3.6 | 5 | 0.1 | 0.60 | 46.5 | 2.59 | 60.7 | 3.82 | 85.1 | 6.41 | 1.87 | 100.7 | 2.97 | 9.98 |
| −4.0 | 1 | 0.4 | 1.03 | 46.7 | 2.62 | 59.8 | 3.93 | 84.1 | 6.55 | 1.52 | 93.2 | 2.81 | 10.39 |
| −4.0 | 2 | 0.3 | 0.99 | 49.0 | 2.63 | 62.5 | 3.83 | 86.4 | 6.46 | 1.72 | 98.8 | 2.86 | 10.31 |
| −4.4 | 1 | 0.4 | 1.07 | 46.6 | 2.57 | 58.6 | 4.03 | 82.5 | 6.60 | 1.41 | 92.1 | 2.77 | 10.44 |
| −4.4 | 2 | 0.4 | 1.02 | 48.8 | 2.56 | 62.0 | 3.83 | 85.5 | 6.39 | 1.73 | 97.7 | 2.90 | 10.31 |

(a) A mean value of $\Delta m_1 = 1.06 \pm 0.04\%$ is obtained in the runs performed at 1°C/min. This value is in fair agreement with the 'conventional' one of 1.13%. Such an agreement becomes worse when a heating rate of 2 or 5°C/min is applied. Indeed, despite the high-resolution intervention, the actual

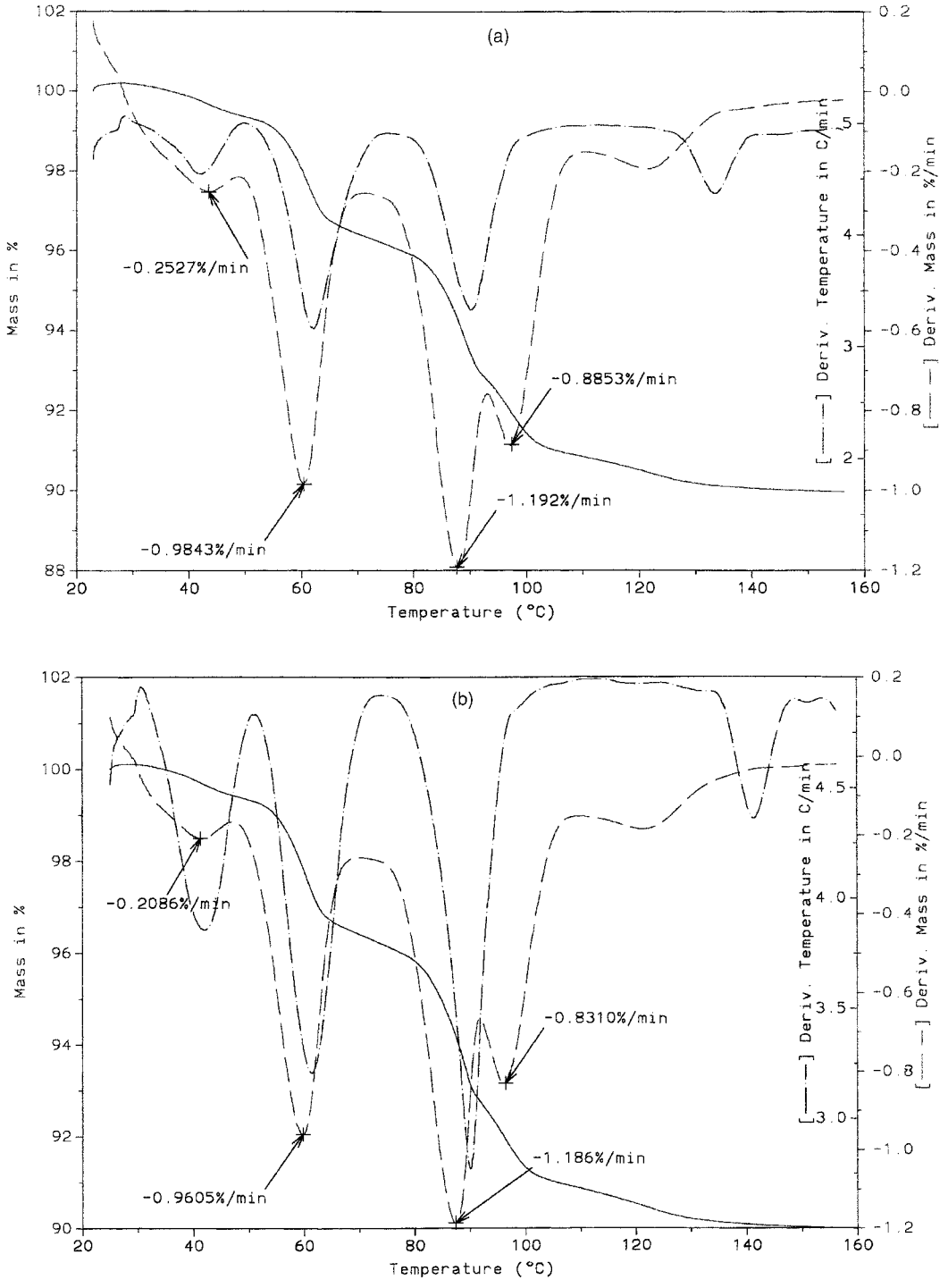


Fig. 5. TGA scans of $\alpha$CD (high resolution-constant reaction rate mode). % Mass, Derivative Mass (%/min) and dynamic heating rate (°C/min). Resolution parameter: $R=-2.7$ (a); $-3.0$ (b); $-3.3$ (c); $-3.6$ (d); $-4.0$ (e). Nominal heating rate: 5°C/min. (f) reports a conventional TGA scan at 5°C/min.

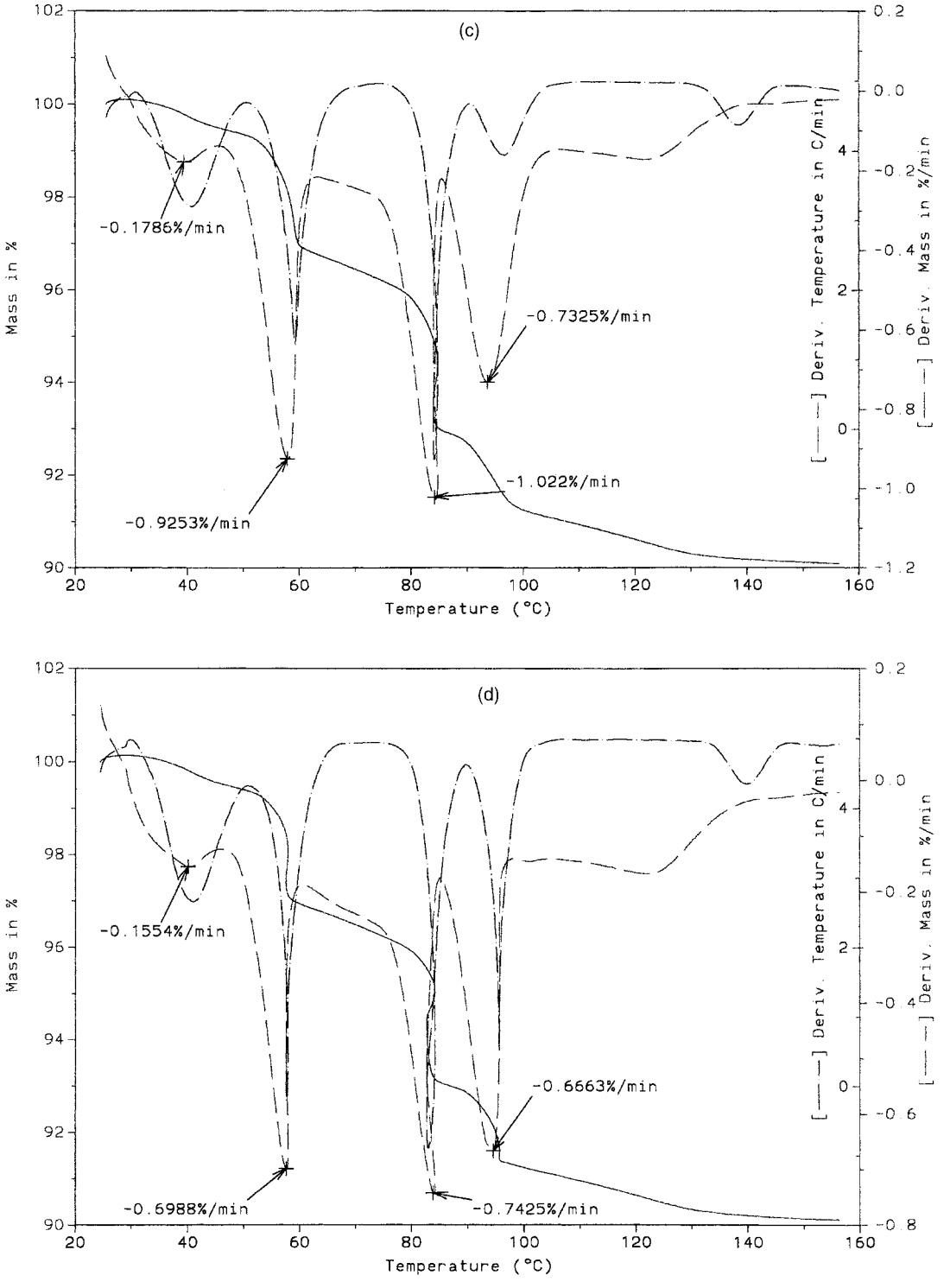


Fig. 5. *(Continued)*

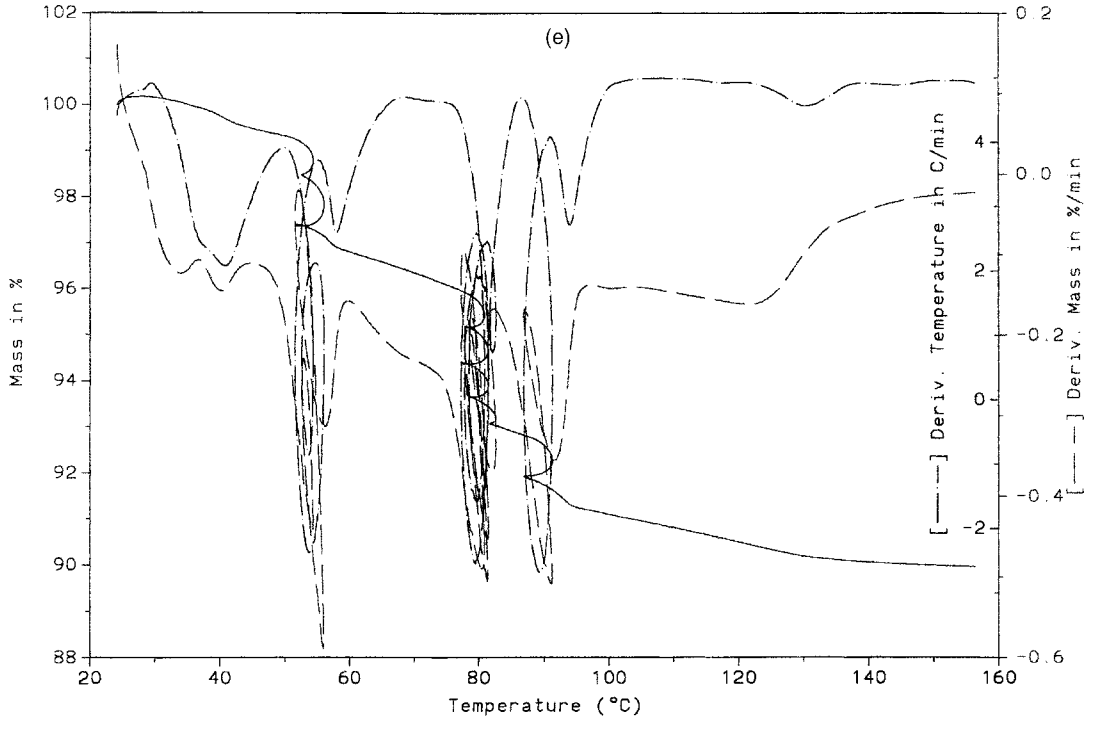


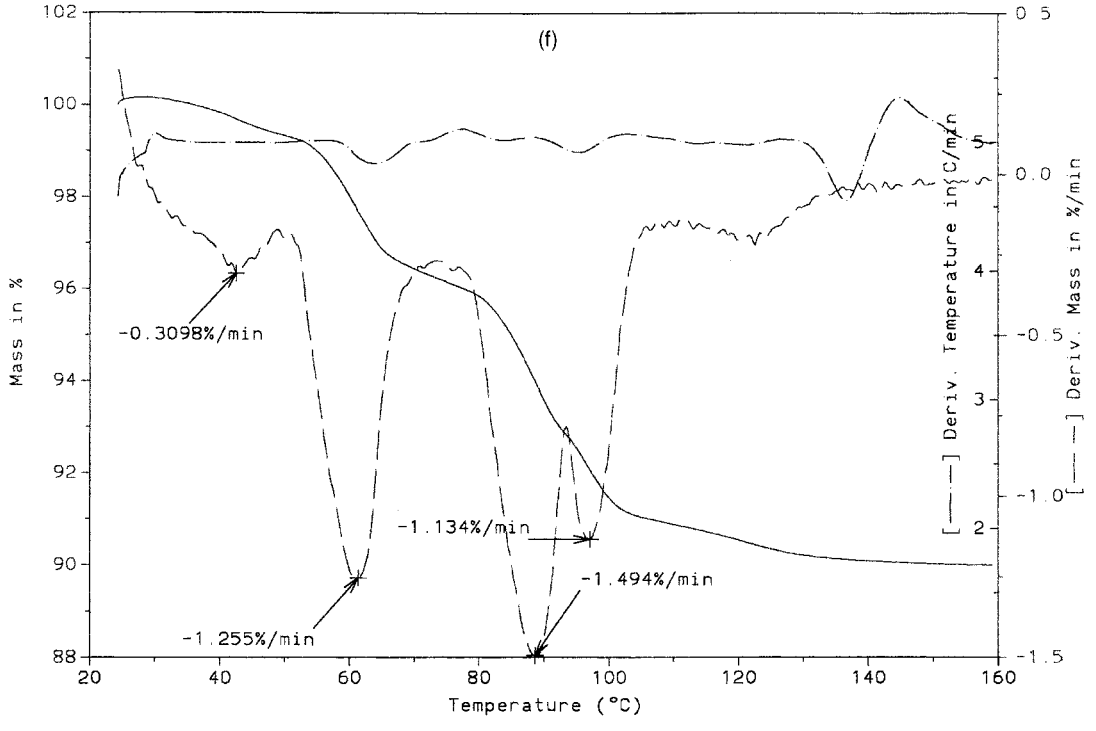


Fig. 5. *(Continued)*

heating rate is always higher than 1°C/min. Therefore, it can be concluded that the resolution of stage 1 is better accomplished by a conventional TGA scan performed at 1°C/min.

(b) Concerning stage 2, it can be seen that in all but two cases ($R=-2.7$ and $R=-3.0$ with $\beta=5$°C/min), the $\Delta m_2$ values are rather well clustered around the mean value ($\Delta m_2=2.62\pm0.05\%$), irrespective of the heating rate. This value is slightly higher than those obtained in the conventional runs at the lowest heating rates, but lower than those obtained at heating rates higher than 1°C/min. Therefore, it can be concluded that the constant reaction rate mode is able to obtain a fair resolution of stage 2 at heating rates (2 and 5°C/min) where such a resolution failed in the conventional mode.

(c) The same considerations, made for stage 2, apply to stage 3. In the two cases mentioned under item (b), $\Delta m_3$ values are lower than the mean value over all other runs ($\Delta m_3=3.89\pm 0.06\%$). Such a value is slightly lower than those obtained by the conventional mode for $\beta\leq0.5$°C/min and, as for stage 2 , it equals the value obtained at 1°C/min. Again, it can be concluded that the constant reaction rate mode gives a better resolution than the conventional one at high heating rates.

(d) At 1°C/min, the mean value of $\Delta m_4$ is $1.49\pm0.08\%$ which is not much different from the values obtained at $\beta\leq1$°C/min in conventional TGA runs. Concerning the runs performed at 2 and 5°C/min, the mean values are $1.66\pm0.09\%$ and $1.93\pm0.05\%$ respectively. These values, despite the high-resolution intervention, are only slightly lower than those obtained by conventional TGA at the same heating rate (see Table 1). Thus, it seems that there is no point in applying high-resolution TGA to resolve stage 4 and, as in the case of stage 1, a conventional run performed at $\beta=1$°C/min or lower would be a better choice.

(e) As expected, the combination of stages 2+3 and 4→ gives $\Delta m_{2+3}=6.52\pm0.08\%$ and $\Delta m_{4\rightarrow}=2.81\pm0.10\%$, which are very close to the corresponding values obtained by both the conventional TGA and Hi-Res™ dynamic range TGA.

## 4. Conclusions

The aim of separating the different stages of αCD dehydration has been pursued by a careful TGA analysis performed both in the conventional and high-resolution modes.

The results we obtained by these different approaches along with the time needed for the runs are summarized in Table 4.

Summarising, the same results have been obtained by conventional TGA performed at $\beta$ <1°C/min and by Hi-Res™ dynamic rate TGA ($R$, 5 to 6, $\beta$, 5–10°C/min). However, the situation is slightly different so far as the constant reaction-rate approach is concerned, where about 0.1% mass loss is shifted from stage 3 to stage 2 and also the resolution of stage 4 is more cumbersome. May be, such an approach is not well suited for the task of resolving the different steps of αCD dehydration. Nevertheless, work is planned to try and apply this mode to another experimental case: the dehydration of γ-cyclodextrin, which is presently under study.

Finally, some comment is worthwhile on the dehydration scheme of αCD outlined in the present study. Apart from the surfacial water (stage 1), the dehydration patterns of αCD can be interpreted as follows:

(a) About 4 water molecules (involving a mass loss of 6.60%) are lost over stages 2 and 3 (total mass loss ca. 6.50–6.55%). It is likely that these water molecules are bonded interstitially to the αCD substrate [7].

(b) About 1.74 water molecules (involving a mass loss of 2.84%) are lost over stage 4 and the

Table 4
Schematic comparison of the results obtained by the different TGA modes (column 1). The symbols stand for the same quantities as in previous tables

| Mode | $\Delta m_2$ | $\Delta m_3$ | $\Delta m_{2+3}$ | $\Delta m_4$ | $\Delta m_{4\rightarrow}$ | Time/min |
|---|---|---|---|---|---|---|
| Conventional $\beta$<1°C/min | 2.48±0.04 | 3.99±0.02 | 6.50±0.03 | 1.57±0.07 | 2.84±0.05 | 280–700 |
| Dynamic rate $R=5\div6$ | 2.51±0.07 | 4.03±0.08 | 6.54±0.09 | 1.54±0.10 | 2.80±0.08 | 35–100 |
| Constant rate $\beta$=1, 2; R=−2.7 to −4.4 | 2.62±0.05 | 3.89±0.06 | 6.52±0.08 | 1.58±0.12 | 2.81±0.10 | 75–200 |

following continuous mass loss process, while ca. 0.7 water molecules are lost at higher temperature (ca. 270°C). These 2.5 water molecules are possibly held in the αCD cavity [7].
(c) The fact that stages 2, 3 and 4 can be resolved, as it has been shown in the present work, either by performing the TGA scan at a low heating rate ($\beta$<1°C/min) or by a suitable use of high-resolution thermogravimetry, could be of interest in revealing subtle differences (e.g. in water bond energy) both in the interstitial (stages 2 and 3) and in the cavity contained (stage 4) water molecules.

Work is in progress by simultaneous TGA/DSC analysis of the αCD dehydration process to gain insight on these interesting aspects.

## References

[1] See for example: M.L. Bender, M. Komiyana, Cyclodextrin Chemistry, Springer Verlag, Berlin 1978; W. Saenger, Angew. Chemie Int. Ed. Engl. 17 (1978) 694.
[2] A. Marini, V. Berbenni, V. Massarotti, P. Mustarelli, R. Riccardi, A. Gazzaniga, F. Giordano, G. Bruni, M. Villa, Solid State Ionics 63–65 (1993) 358.
[3] A. Marini, V. Berbenni, G. Bruni, V. Massarotti, P. Mustarelli, M. Villa, J. Chem. Phys. 103 (1995) 7532.
[4] A. Marini, V. Berbenni, G. Bruni, R. Riccardi, M. Villa, J. Thermal Anal. 50 (1997) 137.
[5] S. Kohata, K. Jyodoi, A. Ohyoshi, Thermochim. Acta 217 (1993) 187.
[6] A. Marini et al., to be published.
[7] K. Lindner, W. Saenger, Acta Cryst. B38 (1982) 210.